

## Instantaneous Impedance Analysis of Non-Stationary Corrosion Process: a Case Study of Carbon Steel in 1M HCl

Jacek Ryl<sup>1,\*</sup>, Lukasz Gawel<sup>1</sup>, Mateusz Cieslik<sup>1</sup>, Husnu Gerengi<sup>2</sup>, Grzegorz Lentka<sup>3</sup>, Pawel Slepiski<sup>1</sup>

<sup>1</sup> Department of Electrochemistry, Corrosion and Materials Engineering, Gdansk University of Technology, Narutowicza 11/12, 80-233 Gdansk, Poland

<sup>2</sup> Corrosion Research Laboratory Department of Mechanical Engineering, Duzce University, 81620, Düzce, TURKEY

<sup>3</sup> Department of Metrology and Optoelectronics, Gdansk University of Technology, Narutowicza 11/12, 80-233 Gdansk, Poland

\*E-mail: [jacek.ryl@pg.gda.pl](mailto:jacek.ryl@pg.gda.pl)

Received: 21 March 2017 / Accepted: 2 May 2017 / Published: 12 June 2017

---

The paper concerns the problem of evaluation of stationarity of carbon steel corrosion in 1M HCl. Comparison of corrosion rate with addition of corrosion inhibitor to the reference measurement is the most often used way of evaluating inhibitor efficiency. Such an approach is valid only if corrosion rate is a stationary process. Two complementary techniques were used simultaneously: volumetric analysis of evolved hydrogen and instantaneous impedance spectroscopy monitoring. Changes of the electrode surface area and chemical composition have a major impact on the dynamics of both cathodic and anodic processes. On the base obtained results, authors claim that the stationarity of the process determined most often on the base of corrosion potential is ineffective and insufficient.

---

**Keywords:** corrosion, carbon steel, impedance monitoring, volumetric analysis

### 1. INTRODUCTION

Carbon steel is the most common construction material, used in all industries. Before its application, a very important role is the treatment of steel with hydrochloric acid, wherein multiple processes are carried out, such as: etching, pickling, descaling, acid cleaning and oil-well acidizing [1]. Various kinds of chemical compounds are investigated for corrosion inhibition effect in order to reduce corrosion rate in such an aggressive environment. Inhibitor efficiency, the main parameter that determines application of these compounds is determined on the base of corrosion rate of steel in hydrochloric acid medium with and without addition of the inhibitor. Usually the values of corrosion

current  $i_{\text{corr}}$ , polarization resistance  $R_p$  or charge transfer resistance  $R_{\text{ct}}$  are being compared. Recently, due to development of impedance techniques, the use of  $R_{\text{ct}}$  is significantly more popular. In order to determine the value of charge transfer resistance one usually utilize the increasingly popular Electrochemical Impedance Spectroscopy (EIS) technique [2-9], which provides multiple information about the system under investigation, such as: time required to achieve the effect of inhibition [10-11], influence of temperature [12] and mechanism of the corrosion process [13-16]. Alternatively, related parameters such as noise resistance  $R_n$  are being compared [17].

Literature reports presenting inhibitor efficiency on base of charge transfer resistance measurements are based on one common assumption, which is constant value of corrosion rate of carbon steel in investigated electrolyte (hydrochloric acid). Reference measurements in the absence of corrosion inhibitor are usually made after certain period of time or after stabilization of corrosion potential value. However, such an approach is only valid if the corrosion rate of carbon steel is a stationary process, otherwise inhibitor efficiency will contain measurement errors. Similarly, small changes in corrosion potential are not meaningful to describe stationary conditions.

Authors want to pay attention to importance of the non-stationarity problem of corrosion process. Many papers dealing with carbon steel corrosion and its inhibitors assume in advance the stationarity of investigated system or the problem is neglected altogether. In the case of corrosion of carbon steel in HCl, time of measurement and time of system stabilization are significant. Reports not taking this into account are not comparable, as they may contain high measurement errors. Two independent techniques were involved in order to resolve the above mentioned problem; volumetric study which allows determination of instantaneous corrosion rate from the amount of evolved hydrogen, and instantaneous impedance measurement which offers the opportunity of on-line monitoring of charge transfer resistance. As a result, it was possible to determine changes of the corrosion process of carbon steel in HCl, and possible causes of the changes during all time of exposition.

## 2. EXPERIMENTAL

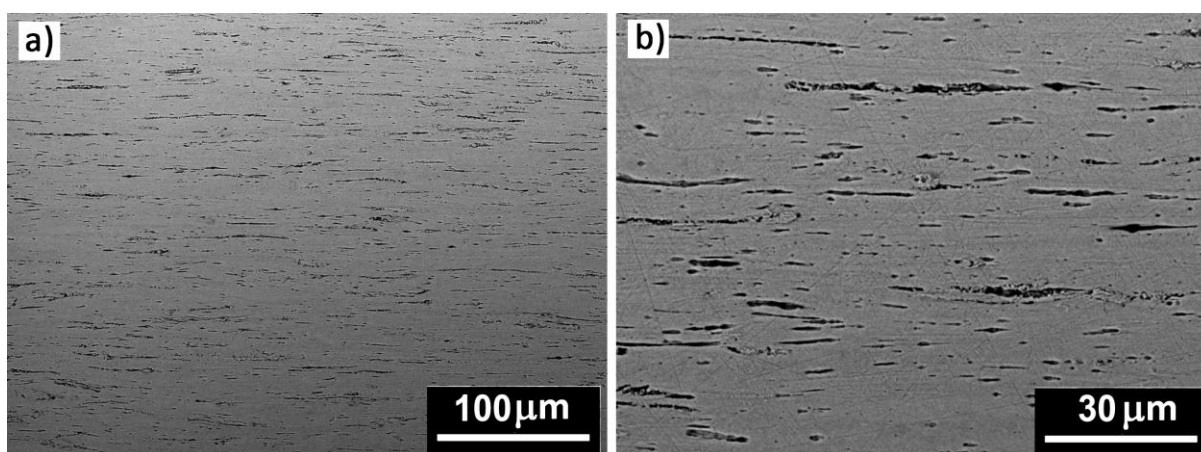


**Figure 1.** SEM micrographs in backscattered electron mode of polished carbon steel sample; a) magnification x300, b) magnification x1000.

Carbon steel wire with diameter of 1.8 mm was used as a working electrode. Its chemical composition is shown in Table 1. To obtain carbon steel microstructure, wire was polished and etched with 3% natal, see Fig. 1.

Micrographs were obtained with backscattered electron (BSE) mode. Microstructure of pearlite (darker) in low carbon matrix has been deformed during wire drawing. The content of pearlite is relative small and crystals are distorted in one direction [18]. The investigated geometrical surface area was 3.9 cm<sup>2</sup>. Prior to experiment sample was mechanically grinded on wet SiC paper (600, 800, 1200, 2000) washed with distilled water, degreased in methanol, and finally dried at room temperature and weighted before being immersed in the acid solution. The aggressive solution (1.0 M HCl) was prepared by diluting analytical grade 37% HCl with distilled water. The solution was saturated with H<sub>2</sub> and brought to the required temperature prior to measurement.

**Table 1.** Chemical composition (wt. %) of investigated carbon steel sample, measured by EDX.

Fe	C	Cu	Si	Ni	Cr	Mn
97.8	0.3	0.3	0.3	0.1	0.1	1.1

Measurements were performed in a thermostatic chamber containing three electrodes: working, reference Ag|AgCl and counter platinum mesh. The temperature was kept at 37 °C. Hydrogen evolved during the exposure was caught in the burette located over the working electrode, which allowed to measure volume of evolved gas as a function of time.

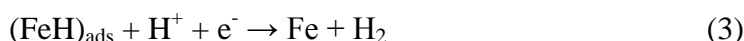
The instantaneous impedance measurement was performed in galvanostatic mode, assuring  $I_{dc}$  was equal to 0. This way, general corrosion conditions were fulfilled. Impedance perturbation signal consisted of multi-sine wave with frequency components between 4.5 kHz and 0.3 Hz and each elementary amplitude selected to assure that overall amplitude of resulting voltage signal does not exceed 20 mV, peak-to-peak. Generation and acquisition of signal were carried out in system consisting of a fast home-made galvanostat and PXI 4464 (National Instruments, Hungary) data acquisition card. The acquired data was analysed with discrete short-time Fourier transformation (DSTFT) to obtain instantaneous impedance spectra as a function of time. In DSTFT time and frequency are discretized. Detailed information about data analysis with DSTFT was presented by Slepki and co-workers [19]. Such an approach has been successfully applied for investigation of various electrochemical and corrosion processes [20-22], however attempts to resolve the problem of non-stationarity during impedance measurements were made already in the 90s of the last century [23].

The effects of steel corrosion in HCl environment was investigated using SEM microscopy and X-ray photoelectron spectroscopy (XPS) techniques. S-3400N SEM microscope (Hitachi, Japan) served to determine topography changes caused by corrosion. Secondary and backscattered electron modes were used at accelerating voltage equal to 20 kV. Detailed analysis of sample chemical composition changes was performed on the basis of XPS with Escalab 250Xi (ThermoFisher Scientific, United Kingdom) equipped in monochromatic Al X-Ray source. High resolution spectra

were acquired at a pass energy of 10 eV and energy step size of 0.1 eV. X-ray spot size was 200  $\mu\text{m}$ . In order to normalize the spectroscopic measurements, X axis (binding energy) from XPS spectrum was calibrated for peak characteristics of neutral carbon C1s (284.6 eV).

### 3. RESULTS AND DISCUSSION

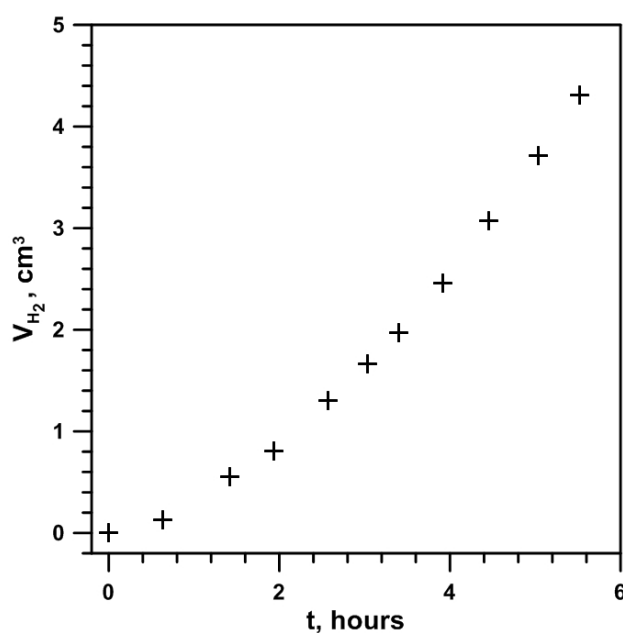
Iron corrosion process in hydrochloric acid environment is composed of two electrode reactions: cathodic hydrogen evolution reaction (HER) and anodic dissolution of iron. Following stages of HER can be distinguished [13,14]:



The chemistry of anodic reaction is not as clear. Some researchers postulate to include various intermediates, such as  $\text{FeOH}_{\text{ads}}$  or  $\text{FeCl}_{\text{ads}}$  [2,14]. Regardless of the exact mechanism, the amount of hydrogen evolved during corrosion of carbon steel in the hydrochloric acid is proportional to the amount of dissolved iron. Simplified reactions are presented below.



Hydrogen collection is well established as a volumetric technique having multiple advantages in corrosion science, in particular in the case of aluminum, magnesium and their alloys [24-29]. Therefore, it is possible to utilize HER to determine changes in weight loss of investigated sample or value of corrosion current with measurement duration.



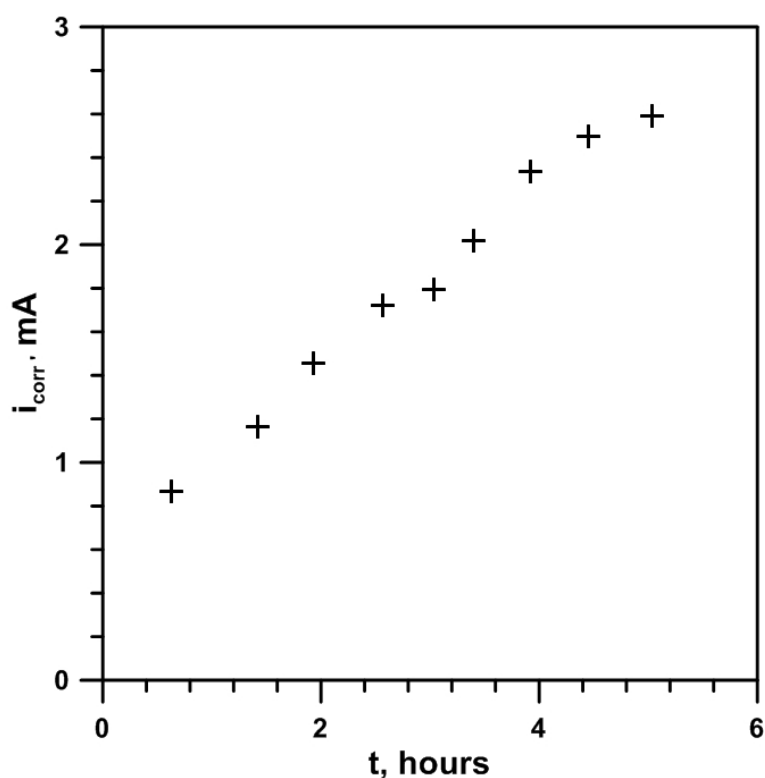
**Figure 2.** Volume of exuded hydrogen changes over time of exposure

Fig. 2 presents measured volume of evolved hydrogen  $V_{H_2}$  during carbon steel exposure in hydrochloric acid. Evolved hydrogen amount is not linear, which might suggest changes of corrosion rate over time of the experiment. Further on,  $V_{H_2}$  from HER was correlated with total weight loss of the sample in order to verify reliability of the measurement. For this purpose equation (6) was used:

$$m = \frac{pVM}{RT} \quad (6)$$

where  $p$  is the gas pressure,  $M$  is the molar weigh,  $R$  is the molar gas constant and  $T$  is the absolute temperature [30].

During 6 hours of the experiment,  $V = 4.31 \text{ cm}^3 \text{ H}_2$  was produced. Total sample weight loss ( $m$ ) equal to 0.0095 g was calculated using eq. (6). On the other hand, measured sample weight loss (difference of carbon steel sample weight before and after exposure) was 0.0100 g. Thus, it may be concluded that the amount of evolved hydrogen  $H_2$  can be treated as a representative parameter for corrosion rate monitoring in this particular case. It should be taken into account that other processes, such as local stirring caused by growth and detachment of hydrogen bubbles might also affect corrosion rate.



**Figure 3.** Changes of corrosion current ( $i_{corr}$ ) over time of exposure.

Changes of  $i_{corr}$  with time are shown on Fig. 3. The value of corrosion current depends on the amount of hydrogen produced, on the base of eq. (4-5). Therefore, the instantaneous value of  $i_{corr}$  during course of the experiment can be calculated from the amount of produced hydrogen using eq. (7) [30]:



$$i_{corr} = \frac{2p\Delta VF}{\Delta t RT} \tag{7}$$

where,  $\Delta t$  is the exposure length and  $F$  is the Faraday constant.

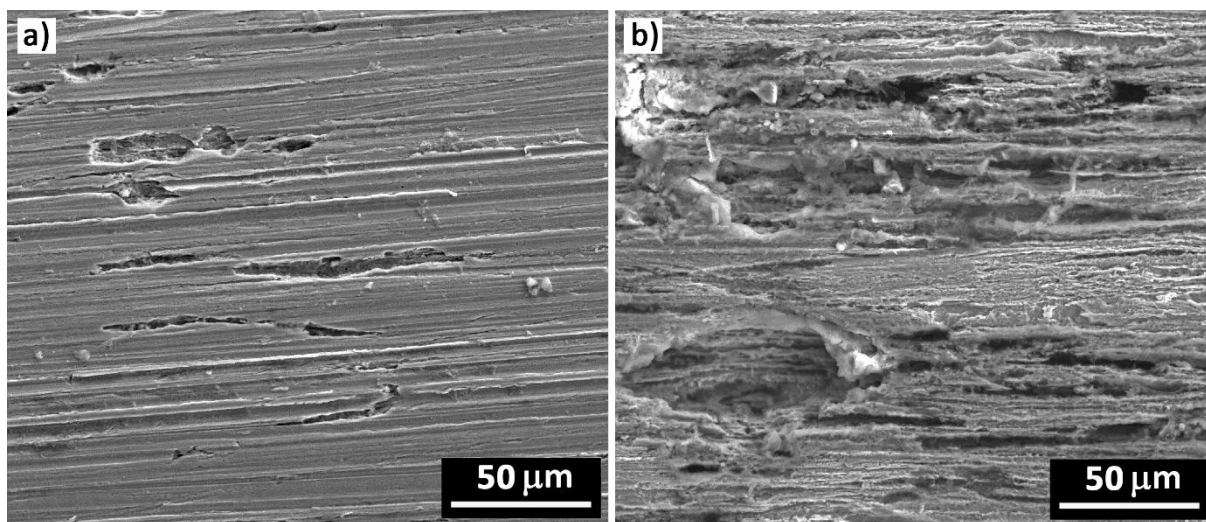


**Figure 4.** SEM micrographs of sample a) before the exposure and b) after 6 h exposition in 1M hydrochloric acid. Secondary electron mode. Magnification x500.

Corrosion current depends on the surface area of investigated sample:  $i_{corr} = f(S)$ . Its value should be constant, with the assumption that the process is stationary and surface area does not expand. In the present case, uniform mass loss of cylindrical sample should result in decrease of the surface area. Instead, SEM micrographs (Fig. 4) demonstrate surface area development under the corrosion process of investigated carbon steel sample. The area of corrosion attack is similar to the shape of pearlite structure in material, hence suggesting that active sites are distributed in vicinity of this phase. Following anodic dissolution of surrounding ferrite, pearlite grains may be detached by evolved hydrogen leaving large caverns (Fig. 4b). These changes also affect the value of impedance of investigated electrode.

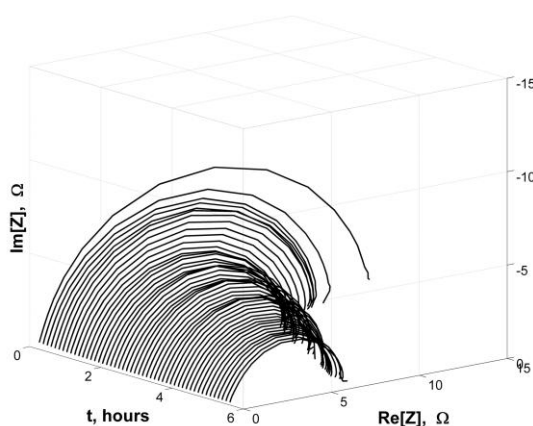


**Figure 5.** Instantaneous impedance spectra in the form of Nyquist plot, 3D projection over time of exposure.

Fig. 5 show instantaneous impedance spectra acquired from DEIS in Nyquist projection versus elapsed experiment time. The spectra has the shape of flattened semicircles with one visible time constant. It can be seen, that semicircular spectra decrease and flatten over time. After 6 hours of measurement, impedance decreased almost twice. In the stationary process, impedance should not change in time. Changes can be caused by modification of surface area or increased rate of corrosion process rate as was mentioned earlier. However, to address the source of these changes, an impedance spectra analysis is necessary. To estimate the value of charge transfer resistance one is obliged to perform fitting procedure with an electric equivalent circuit, while the circuit must offer good physical explicability. The availability of hydrogen ions, a depolarizer in the investigated process, as well as mixing of the electrolyte by detaching hydrogen bubbles practically eliminates the influence of diffusive transport. The corrosion reaction is controlled through the charge-transfer process. For this reason, the impedance spectra obtained for carbon steel in hydrochloric acid are commonly processed with the use of  $R_1(Q_2R_3)$  electric equivalent circuit [6,12,15]. Here,  $R_1$  represents electrolyte resistance,  $R_3$  charge transfer resistance  $R_{CT}$  and  $Q$  is the constant phase element (CPE), often introduced to evaluate double-layer capacitance  $C_{dl}$ , dispersed due to surface heterogeneities [32]. Unlike  $i_{corr}$ ,  $R_{CT}$  is inversely proportional to the changes of surface area,  $1/R_{CT}=f(S)$ , as can be seen on Fig. 6. Similarly, growth of double-layer capacitance also testifies surface area development of investigated sample, assuming limited influence of adsorbed reaction intermediates. Its effective value,  $C_{eff}$ , was estimated from CPE on the base of surface distribution model proposed by Hirschorn and co-workers [33].

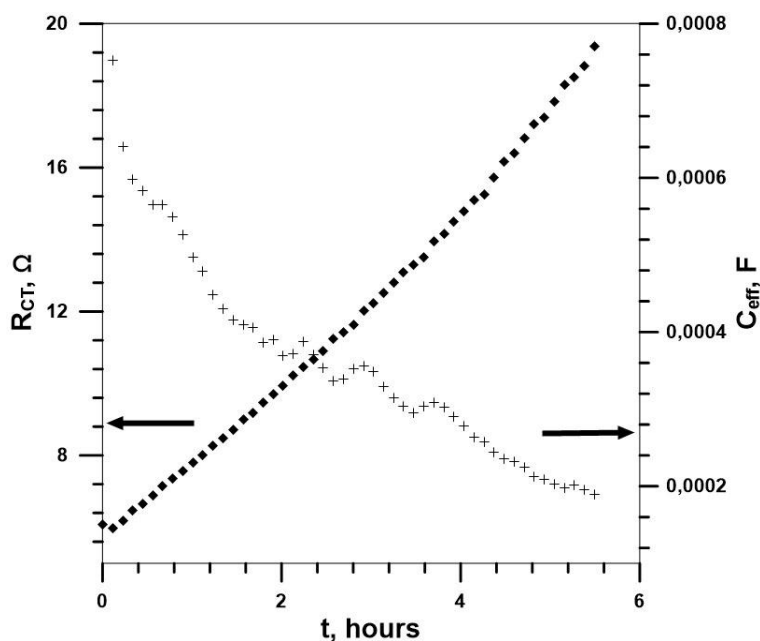


**Figure 6.** Charge-transfer resistance ( $R_{CT}$ ) and effective double-layer capacitance ( $C_{eff}$ ) changes over time of exposure. Estimated from instantaneous impedance spectra on the base of fitting procedure with  $R(QR)$  equivalent circuit.

It is essential to determine the change of surface area during course of experiment or to eliminate this factor altogether to be able to determine whether corrosion rate was affected by factors other than just surface area development. Estimation of surface area development is extremely complex, however there is a way to neglect its influence. To do so, authors utilize Stern-Geary formula (8), which links charge transfer resistance  $R_{CT}$  with corrosion current  $i_{corr}$  [34, 35]:

$$i_{corr} = \frac{b_a b_c}{2.303(b_a + b_c)} \frac{1}{R_{CT}} = \frac{B}{R_{CT}} \quad (8)$$

where  $b_a, b_c$  are anodic and cathodic Tafel slopes, respectively.

Surface area of investigated sample determines both the instantaneous value of corrosion current as well as instantaneous value of charge transfer resistance. On the other hand,  $B$  parameter calculated from eq. (9) is surface area independent. It represents mechanism and kinetics of both the anodic and the cathodic processes.

$$B = i_{corr} f(S) \cdot 1/R_{CT} f(S) \quad (9)$$

The changes of  $B$  parameter calculated from instantaneous values of  $R_{CT}$  and  $i_{corr}$  are shown on Fig. 7. It should be observed, that the course of  $B=f(t)$  tends to increase in the range between 13 mV/dec to around 20 mV/dec at the end of the experiment.

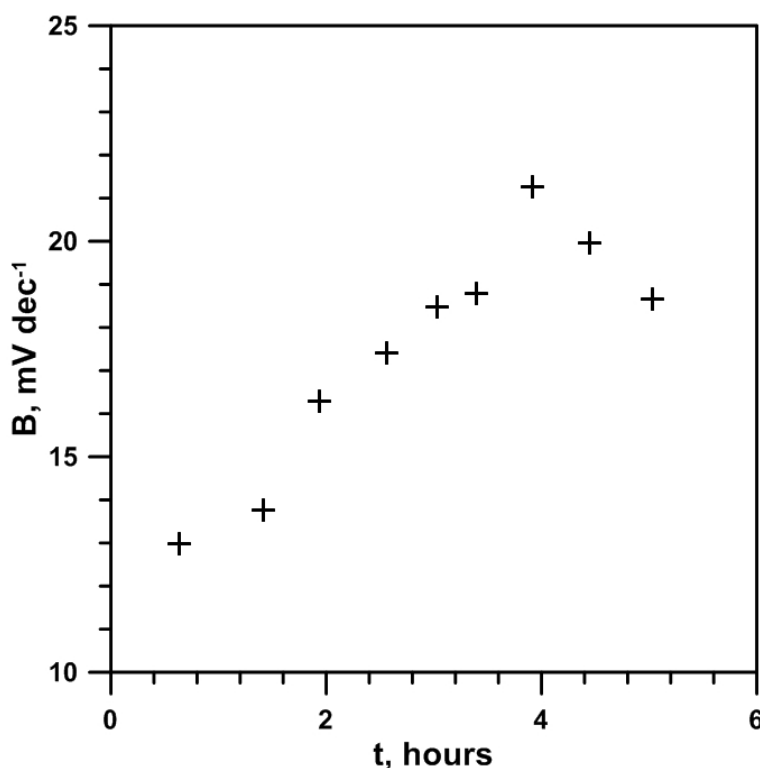


**Figure 7.**  $B$  parameter changes over time of exposure, calculated using eq. (9).

Numerous research articles on topic of carbon steel corrosion in 1M HCl show a very large discrepancies of this parameter, where the value of anodic slope  $b_a$  is typically in range between 66-140 mV/dec and cathodic slope  $b_c$  is between 77-246 mV/dec, thus  $B$  is in range from 17.1 to 37.5 mV/dec [3,5,6,8,9,12,14,16]. Vast discrepancies reach beyond the effect of temperature variations or



slight changes in chemical constitution between investigated carbon steel samples. Therefore, authors claim that observed discrepancy originates from different (unstandardized) duration of reference measurements to estimate the corrosion rate, while the control of this factor is essential to evaluate nonstationary processes, such as carbon steel corrosion in hydrochloric acid.

There are three possible explanations to  $B$  increase on the base of eq. (8): (I) individual increase of  $b_a$ , (II) individual increase of  $b_c$  and (III) simultaneous increase of both  $b_a$  and  $b_c$ . In each case, decrease of corrosion current density and corrosion rate with respect to real surface area, is to be expected. In addition, if only a single slope is affected, as is in cases (I) and (II), the additional effect will be the change of the corrosion potential  $E_{corr}$  while changes of corrosion potential  $E_{corr}$  registered throughout the experiment are negligible, not exceeding 6 mV (Fig. 8). Authors findings corroborate with literature data, most often the reports for carbon steel in hydrochloric acid show no significant changes of corrosion potential [3,5,8,9]. Thus, it should be concluded that both anodic as well as cathodic processes are affected. Such behaviour may be caused by changes of alloy surface chemistry during exposure to hydrochloric acid.

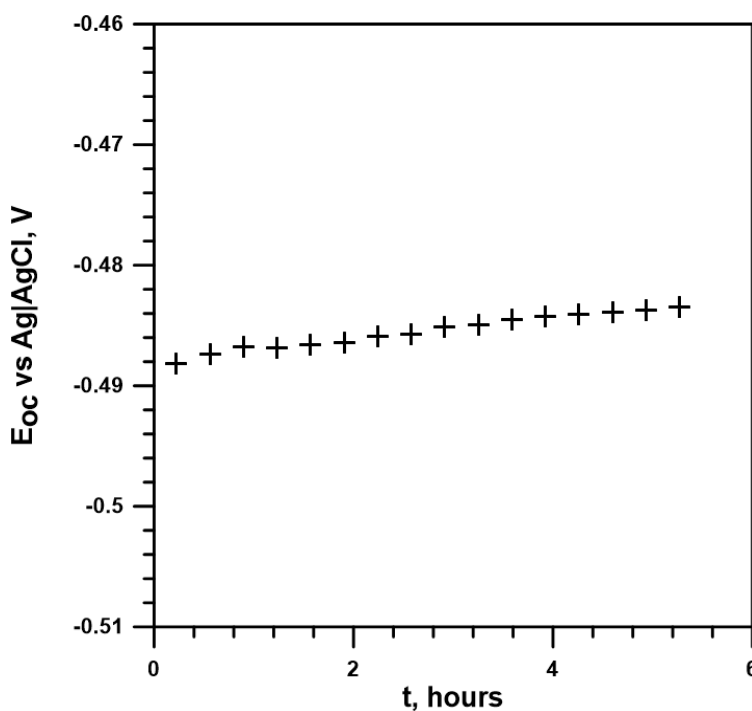


**Figure 8.** Changes of corrosion potential ( $E_{corr}$ ) over time of exposure.

XPS analysis has shown a meaningful change of the chemical composition of investigated sample. The analysis was performed after etching with an ion gun (200s, 3000V) to remove major surface contamination from atmospheric air. The chemical composition (in %wt) is given in Table 2. As a result of exposure to hydrochloric acid the relative share of iron has decreased by 20% with an increase of relative share of alloying additives as well as carbon by up to 15%. It was observed that corrosion process is selective for iron and does not include alloying elements of cathodic nature. Relatively high share of carbon and oxygen can be justified by hindered removal of oxide layer and

contaminations from rough electrode surface. In particular the chemistry of high-resolution XPS spectra for C1s has changed, as presented on Fig. 9. XPS spectra for reference sample (before immersion) can be deconvoluted into two components; main located at binding energy of 284.8 eV as is typical for C-C aliphatic bonds and second component shifted by +1.1 eV for C-O bonds. Both of these originate from atmospheric air exposure. As a result of immersion in hydrochloric acid a third component appears in C1s spectra, at ~283.6 eV. The indicated energy is characteristic for Fe<sub>3</sub>C [36,37].

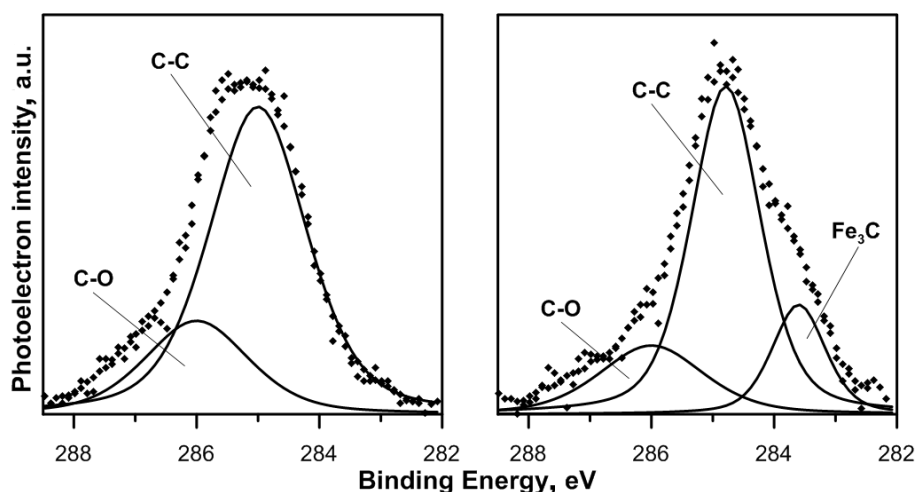


**Figure 9.** High-resolution XPS spectra recorded for C1s region before the experiment and after 6 h exposure in 1M HCl.

**Table 2.** Chemical composition (at. %) on the surface of carbon steel sample, obtained from XPS.

	Fe	Cu	Si	C	O
Before the experiment	87.5	< 0.5	< 0.5	8.4	4.1
After 6h in 1M HCl	64.1	1.3	1.7	26.0	6.9

Demonstrated composition changes have a significant influence on the mechanism of electrode processes. The amount of iron starts to decrease, with increase of copper, silicon and carbon most likely in the form of carbides. This has impact on HER overpotentials and possible intermediates of anodic and cathodic processes, however understanding nature of these changes require additional studies.

#### 4. CONCLUSIONS

Corrosion of carbon steel in hydrochloric acid is not as simple as it might appear in the first place. The process is not stationary and its nature complex. Corrosion process affects the geometry and the composition of exposed surface. Utilization of on-line instantaneous impedance monitoring in

galvanostatic mode with simultaneous volumetric measurement made it possible to demonstrate that corrosion current density decreases as a result of these changes. Both the anodic and cathodic processes were responsible for change of the corrosion rate of investigated carbon steel.

The discussed changes are not accessible by commonly used free corrosion potential monitoring. In such case, fluctuations of corrosion potential are negligible, which normally is perceived as evidence for stationary conditions. This approach is particularly inappropriate if corrosion of carbon steel in hydrochloric acid is treated as reference for determination of inhibitor efficiency of variable chemical compounds. The result of such study will largely depend on the length of measurement, which should always be taken into account.

#### ACKNOWLEDGEMENT

The authors gratefully acknowledge the financial support from the Polish National Science Centre (NCN) under grant no. 2015/17/D/ST5/02571 and Polish Ministry of Science and Higher Education budget funds in 2016-2019 under Iuventus Plus project IP2015 067574.

#### References

1. G. Schmitt, *Br. Corros. J.*, 19 (1984) 165. <http://dx.doi.org/10.1179/000705984798273100>
2. D. Ben Hmamou, R. Salghi, A. Zarrouk, B. Hammouti, S.S. Al-Deyab, Lh. Bazzi, H. Zarrok, A. Chakir and L. Bammou, *Int. J. Electrochem. Sci.*, 7 (2012) 2361.
3. I. Ahamad, R. Prasad and M.A. Quraishi, *Corros. Sci.*, 52 (2010) 933. <http://dx.doi.org/10.1016/j.corsci.2009.11.016>
4. K. F. Khaled and A.M. Amin, *Corros. Sci.*, 51 (2009) 1964. <http://dx.doi.org/10.1016/j.corsci.2009.05.023>
5. M. Mobin and M. Rizvi, *Carbohydr. Polym.*, 136 (2016) 384. <http://dx.doi.org/10.1016/j.carbpol.2015.09.027>
6. M.A. Hegazy, A.M. Badawi, S.S. Abd El Rehim and W.M. Kamel, *Corros. Sci.*, 69 (2013) 110. <http://dx.doi.org/10.1016/j.corsci.2012.11.031>
7. N. M'hiri, D. Veys-Renaux, E. Rocca, I. Ioannou, N.M. Boudhrioua and M. Ghoul, *Corros. Sci.*, 102 (2016) 55. <http://dx.doi.org/10.1016/j.corsci.2015.09.017>
8. E. A. Noor and A.H. Al-Moubaraki, *Int. J. Electrochem. Sci.*, 3 (2008) 806.
9. Y. Sangeetha, S. Meenakshi and C. Sairam Sundaram, *J. Appl. Polym. Sci.*, 133 (2016) 43004. <http://dx.doi.org/10.1002/app.43004>
10. W.A.W. Elyn Amira, A.A. Rahim1, H. Osman, K. Awang and P. Bothi Raja, *Int. J. Electrochem. Sci.*, 6 (2011) 2998 – 3016.
11. K. C. R. Ferreira, R. F. B. Cordeiro, J. C. Nunes, H. Orofino, M. Magalhães, A. G. Torres and E. D'Elia, *Int. J. Electrochem. Sci.*, 11 (2016) 406 – 418.
12. G. Sığırcık, T. Tüken and M. Erbil, *Corros. Sci.*, 102 (2016) 437. <http://dx.doi.org/10.1016/j.corsci.2015.10.036>
13. A. Döner, R. Solmaz, M. Özcan and G. Kardas, *Corros. Sci.*, 53 (2011) 2902. <http://dx.doi.org/10.1016/j.corsci.2011.05.027>
14. D. K. Yadav and M.A. Quraishi, *Ind. Eng. Chem. Res.*, 51 (2012) 8194. <http://dx.doi.org/10.1021/ie3002155>
15. I. Ahamad, R. Prasad and M.A. Quraishi, *Corros. Sci.*, 52 (2010) 1472. <http://dx.doi.org/10.1016/j.corsci.2010.01.015>

16. L. O. Olasunkanmi, M.M. Kabanda and E.E. Ebenso, *Physica E*, 76 (2016) 109. <http://dx.doi.org/10.1016/j.physe.2015.10.005>
17. J.M. Smulko, K. Darowicki and A. Zielinski, *Russ. J. Electrochem.*, 42 (2006) 546. <http://dx.doi.org/10.1134/S1023193506050132>
18. X. Li, L. Cao, M. Wang and F. Du, *Model. Simul. Mater. Sc.*, 2 (2012) 67. <http://dx.doi.org/10.4236/mnsms.2012.24008>
19. P. Slepski, K. Darowicki, and K. Andrearczyk, *J. Electroanal. Chem.*, 633 (2009) 121. <http://dx.doi.org/10.1016/j.jelechem.2009.05.002>
20. J. Ryl, J. Wysocka, P. Slepski and K. Darowicki, *Electrochim. Acta*, 203 (2016) 388. <http://dx.doi.org/10.1016/j.electacta.2016.01.216>
21. J. Ryl, K. Darowicki, and P. Slepski, *Corros. Sci.*, 53 (2011) 1873. <http://dx.doi.org/10.1016/j.corsci.2011.02.004>
22. H. Gerengi, P. Slepski, E. Ozgan and M. Kurtnay, *Mater. Corros.*, 66 (2015) 233. <http://dx.doi.org/10.1002/maco.201307287>
23. B. Savova-Stoynov and Z.B. Stoynov, *Key Engineering Materials*, 59-60 (1991) 273. <http://dx.doi.org/10.4028/www.scientific.net/KEM.59-60.273>
24. T.R. Thomaz, C.R. Weber, Jr. T. Pelegrini, L.F.P. Dick and G. Knörnschild, *Corros. Sci.*, 52 (2010) 2235. <http://dx.doi.org/10.1016/j.corsci.2010.03.010>
25. D. Eaves, G. Williams and H.N. McMurray, *Electrochim. Acta*, 79 (2012) 1. <http://dx.doi.org/10.1016/j.electacta.2012.05.148>
26. S. Fajardo and G.S. Frankel, *Electrochim. Acta*, 165 (2015) 255. <http://dx.doi.org/10.1016/j.electacta.2015.03.021>
27. J. He, B. Jiang, J. Zhang, Q. Xiang, X. Xia and F. Pan, *Mater. Sci. Eng. A*, 647 (2015) 216. <http://dx.doi.org/10.1016/j.msea.2015.09.002>
28. S. Gudić, I. Smoljko and M. Kliskić, *J. Alloy. Compd.*, 505 (2010) 54. <http://dx.doi.org/10.1016/j.jallcom.2010.06.055>
29. E.E. Oguzie, *Resin. Technol.*, 34 (2005) 321. <http://dx.doi.org/10.1108/03699420510630336>
30. B. Lei, M. Li, Z. Zhao, L. Wang, Y. Li and F. Wang, *Corros. Sci.*, 79 (2014) 198. <http://dx.doi.org/10.1016/j.corsci.2013.11.007>
31. A.W. Jun-Bo, W. Jian-Ming, S. Hai-Bo, Z. Jian-Qing and C. Chu-Nan, *J. Appl. Electrochem.*, 37 (2007) 753. <http://dx.doi.org/10.1007/s10800-007-9310-8>
32. S. Ben Aoun, M. Bouklah, K.F. Khaled and B. Hammouti, *Int. J. Electrochem. Sci.*, 11 (2016) 7343. <http://dx.doi.org/10.20964/2016.09.07>
33. B. Hirschorn, M. Orazem, B. Tribollet, V. Vivier, I. Frateur and M. Musiani, *Electrochim. Acta*, 55 (2010) 6218. <http://dx.doi.org/10.1016/j.electacta.2009.10.065>
34. M. Stern and A.L. Geary, *J. Electrochem. Soc.*, 104 (1957) 56. <http://dx.doi.org/10.1149/1.2428496>
35. F. Mansfeld, *J. Solid State Electrochem.*, 13 (2009) 515. <http://dx.doi.org/10.1007/s10008-008-0652-x>
36. H. Goretzki, P.V. Rosenstiel and S. Mandziej, *Fresenius J. Anal. Chem.*, 333 (1989) 451. <http://dx.doi.org/10.1007/BF00572350>
37. D.A. Lopez, W.H. Schreiner, S.R. de Sanchez and S.N. Simison, *Appl. Surf. Sci.*, 207 (2003) 69. [http://dx.doi.org/10.1016/S0169-4332\(02\)01218-7](http://dx.doi.org/10.1016/S0169-4332(02)01218-7)

© 2017 The Authors. Published by ESG ([www.electrochemsci.org](http://www.electrochemsci.org)). This article is an open access article distributed under the terms and conditions of the Creative Commons Attribution license (<http://creativecommons.org/licenses/by/4.0/>).

